Mechanism of UV-Induced Conformational Changes among Enol-Type Isomers of (Trifluoroacetyl)acetone Studied by Low-Temperature Matrix-Isolation Infrared Spectroscopy and Density Functional Theory Calculation

Yukiko Minoura, Naoko Nagashima, Satoshi Kudoh, and Munetaka Nakata*

Graduate School of BASE (Bio-Applications and Systems Engineering), Tokyo University of Agriculture and Technology, 2-24-16 Naka-cho, Koganei, Tokyo 184-8588, Japan

Received: October 28, 2003

UV-induced conformational changes among chelated and nonchelated enol isomers of (trifluoroacetyl)acetone in a low-temperature argon matrix were investigated by Fourier transform infrared spectroscopy. An infrared spectrum measured after deposition before UV irradiation was assigned to a chelated enol isomer, 1,1,1-trifluoro-4-hydroxy-3-penten-2-one, where no bands for the other chelated enol isomer, 5,5,5-trifluoro-4-hydroxy-3-penten-2-one, were found, the latter being formed from the former by moving of the hydrogen atom in the O−H group to the C═O group. Conformations of 3 nonchelated enol isomers among 14 were determined by a comparison of the infrared spectra measured after UV irradiation with the spectral patterns obtained by the density functional theory calculations at the DFT/B3LYP/6-31G* level. This selective isomerization was explained in terms of the inhibition of internal rotation in vibrational relaxation of photoexcited species, which was proposed in our previous studies of acetylacetone and hexafluoroacetylacetone. An infrared spectrum of a transient photoproduct was measured while the matrix sample was continuously exposed to the UV light. It was identified as another nonchelated enol isomer.

Introduction

Acetylacetone (AA) is one of the most fundamental β-diketone compounds and is used as a ligand of a variety of metal complexes.[1,2] In an isolated molecule, however, the keto form is less stable than the enol one, which is strongly stabilized by intramolecular hydrogen bonding of C═O- - -H−O−C. The keto−enol tautomerization in the gas phase and in solution has been investigated by various spectroscopies such as photoelectron,[3] NMR,[4,5] and infrared,[6,7] where the chelated enol form exists mostly (Scheme 1).

On the other hand, it was reported that a few nonchelated enol forms, which are less stable than the chelated enol and keto isomers, were produced by UV irradiation.[8−10] Since the enol form has trans and cis conformations around the three rotational axes, C2−C3, C3═C4, and C4−O5, eight enol isomers are possible. Among the eight isomers, Roubin et al.[8,9] assumed that three nonchelated enol isomers, *cct*, *tcc*, and *tct*, were produced from the most stable chelated enol isomer, *ccc*, by UV irradiation, where the first, second, and last letters, *t* and *c*, denote the trans and cis conformations around the C2−C3, C3═C4, and C4−O5 bonds, respectively. In contrast to their unfounded assignments limited to the central cis conformations, we[10] clearly identified the nonchelated enol isomers produced by UV irradiation as *ctc*, *tct*, and *ttc* by a comparison of the measured infrared spectra with the calculated spectral patterns obtained by the density functional theory (DFT) method,[11,12] which reproduced the vibrational wavenumbers within 20 cm^{-1} if a suitable scaling factor was used.[13−21] Reversible conformational isomerization between the chelated enol and the nonchelated enols in low-temperature matrices was also observed.[22]

* Author to whom correspondence should be addressed. E-mail: necom@cc.tuat.ac.jp. Phone and Fax: +81-42-388-7349.

SCHEME 1

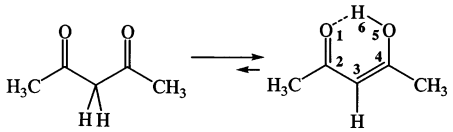

Conformational isomerization for hexafluoroacetylacetone (HFAA)[23,24] was also investigated, where a single nonchelated isomer, *ctt*, was produced from the *ccc* isomer by shorter wavelength UV irradiation (260 nm < λ < 300 nm) and backward conformational isomerization occurred by longer wavelength UV irradiation (320 nm < λ < 340 nm). This reversible photoisomerization between *ccc* and *ctt* was considered to be applicable to a molecular memory or a molecular switch.

In the present study, we have investigated another fluorinated derivative of AA, i.e., (trifluoroacetyl)acetone (TFAA). Contrary to plentiful publications for AA and HFAA, neither spectrum nor vibrational analysis on the photoisomerization of TFAA, to our best knowledge, has been reported. Since the molecular geometry of TFAA is asymmetric unlike AA and HFAA, its conformational changes seem to be more complicated than those of AA and HFAA, where the 16 enol isomers shown in Figure 1 must be taken into account: F-*xxx* and *xxx*-F denote the isomers of 1,1,1-trifluoro-4-hydroxy-3-penten-2-one and those of 5,5,5-trifluoro-2-hydroxy-3-penten-4-one, respectively. Despite much complication of conformational changes due to the existence of many possible isomers, we have tried to measure infrared spectra of less stable isomers produced by UV irradiation and identify their conformations with the aid of DFT calculations. The infrared bands measured in low-temperature argon matrices are so sharp and the calculated spectral patterns

10.1021/jp031192y CCC: $27.50
Published on Web 03/02/2004

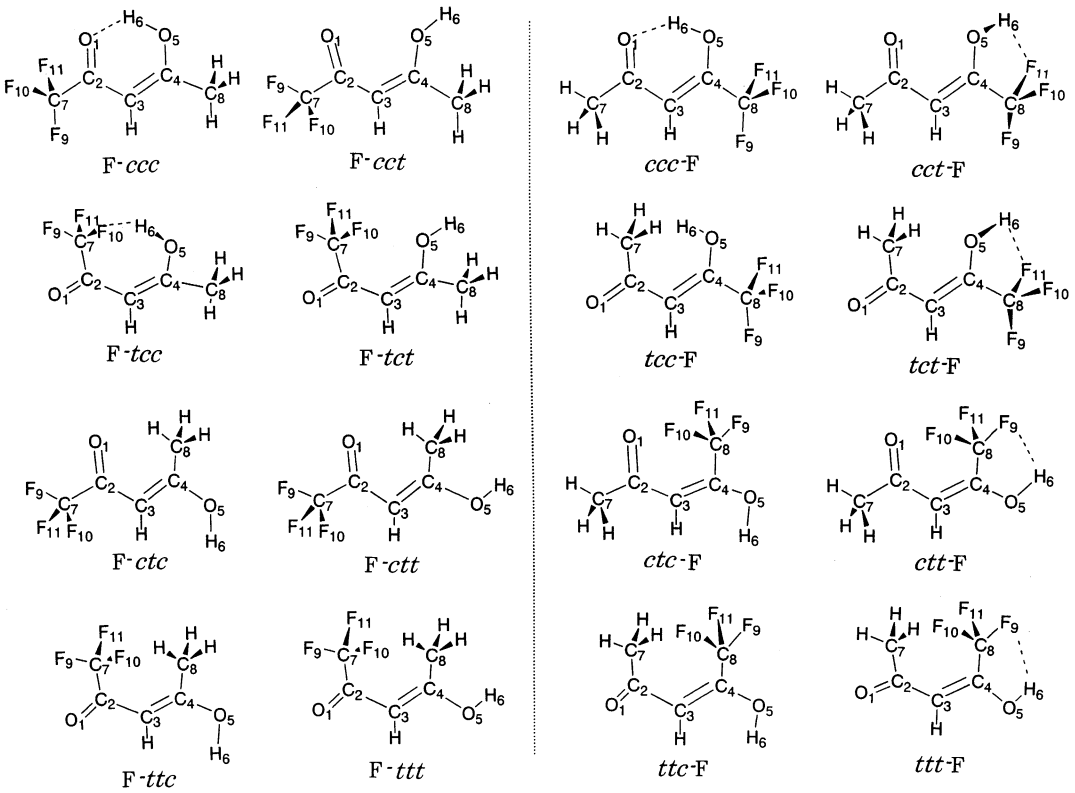

Figure 1. Sixteen possible isomers of enol-type (trifluoroacetyl)acetone and numbering of atoms: isomers of 1,1,1-trifluoro-4-hydroxy-3-penten-2-one and 5,5,5-trifluoro-4-hydroxy-3-penten-2-one are denoted as F-*xxx* and *xxx*-F, respectively. Broken lines represent hydrogen bonding.

obtained by the calculation are so reliable that the isomer bands in the observed spectra are distinguishable from each other. On the basis of the identification and comparison with the results of AA[10] and HFAA,[23,24] we discuss possible mechanisms for conformational changes among the chelated and nonchelated enol isomers caused by UV irradiation.

Experimental Section

A sample of TFAA (more than 98.0% purity), purchased from Tokyo Chemical Industry Co., was used after vacuum distillation after the removal of water by magnesium sulfide. The sample vapor was premixed with argon gas (Taiyo Toyo Sanso, higher than 99.9999% purity) in a glass bulb. The mixing ratio of TFAA/Ar was about 1/2000. The premixed gas was deposited through a stainless steel pipe of 1/8-in. o.d. on a CsI plate at 15 K cooled by a closed-cycle helium refrigeration unit. The pressures in the vacuum chamber were about 1×10^{-5} and 5×10^{-4} Pa before and during the sample deposition, respectively. The deposition time was about 1 h. A superhigh-pressure mercury lamp (Ushio UI-501C) was used as a light source to induce conformational changes. The UV light was introduced to the matrix sample through a water filter of 50-mm diameter and 100-mm length, a quartz lens of 50-mm diameter and 200-mm focus length, and a quartz window of the vacuum chamber. Optical short-cut filters, UV-28, UV30, UV32, UV34, and UV36 (HOYA), were used in experiments for wavelength dependence. Infrared spectra were measured with an FTIR spectrophotometer (JEOL, JIR-7000). The infrared beam of the spectrophotometer was introduced to the matrix sample through a KBr window and detected with a liquid-nitrogen-cooled MCT detector placed on the opposite side of the vacuum chamber. The spectral resolution was 0.5 cm^{-1}, and the number of accumulations was 64. Other experimental details are reported elsewhere.[10,23]

Results and Discussion

Optimized Geometry and Relative Energy. DFT calculations were employed using GAUSSIAN 98 program[25] with the 6-31G* basis set, where the hybrid density functional,[26] in combination with the Lee−Yang−Parr correlation functional (B3LYP),[27] was used to optimize the geometrical structures. The calculated bond distances and angles of the skeletons for the 16 enol isomers shown in Figure 1 and their relative energies are summarized in Table 1. Buemi[28] employed a similar calculation at the DFT/B3LYP/6-31G** level and reported the optimized geometrical parameters of the F-*ccc*, F-*cct*, *ccc*-F, and *cct*-F isomers. His calculated values are consistent with ours to within 0.2%.

The chelated enol isomers, F-*ccc* and *ccc*-F, have intramolecular hydrogen bonding between O−H and C═O groups: The O−H distances, 1.005 and 1.009 Å for F-*ccc* and *ccc*-F, respectively, are longer than those of the other enol isomers, ca. 0.97 Å, while the C═O distances, 1.244 and 1.245 Å, are longer than those of the others, ca. 1.22 Å. The energy difference between F-*ccc* and *ccc*-F is estimated to be 4.68 kJ mol^{-1}, where the corresponding value after the zero-point vibrational correction is 3.40 kJ mol^{-1}. The distances of the C2−C3 and C3═C4 bonds in F-*ccc* are shorter and longer than those in *ccc*-F, respectively, implying that F-*ccc* is stabilized by stronger π-electron conjugation than *ccc*-F. Thus the trifluoromethyl group interacts with the carbonyl group more strongly than the hydroxyl group.

All the nonchelated enol isomers are less stable than the two chelated enol isomers. The order of relative energies in the F-*xxx* group is *ccc* < *ctc* < *tcc* < *ctt* < *cct* < *ttc* < *tct* < *ttt*, while that in the *xxx*-F group is *ccc* < *tct* < *tcc* < *cct* < *ctt* < *ttt* < *ctc* < *ttc*. These orders are different from each other and from that for AA:[10] *ccc* < *ctc* < *ctt* < *tcc* < *tct* < *ttc* < *cct* < *ttt*.

TABLE 1: Optimized Geometry (Bond Lengths, *r*, in Å and Bond Angles, ∠, in deg)[a] and Relative Energy (in kJ mol^{-1}) for 16 Enol Isomers of (Trifluoroacetyl)acetone

	F-*ccc*	F-*cct*	F-*tcc*	F-*tct*	F-*ctc*	F-*ctt*	F-*ttc*	F-*ttt*
ΔE^b	0.0	61.9	47.5	67.9	42.4	48.0	62.1	71.3
r(O1═C2)	1.244	1.218	1.221	1.220	1.221	1.223	1.221	1.221
r(C2−C3)	1.428	1.456	1.454	1.461	1.453	1.452	1.456	1.456
r(C3═C4)	1.379	1.357	1.366	1.356	1.362	1.358	1.362	1.358
r(C4−O5)	1.323	1.348	1.342	1.351	1.350	1.354	1.355	1.360
r(O5−H6)	1.005	0.971	0.973	0.970	0.973	0.971	0.973	0.970
r(C2−C7)	1.543	1.554	1.553	1.553	1.554	1.553	1.552	1.552
r(C4−C8)	1.496	1.502	1.500	1.503	1.494	1.498	1.500	1.502
r(C7−F9)	1.351	1.333	1.324	1.337	1.332	1.334	1.332	1.331
r(C7−F10)	1.341	1.354	1.380	1.349	1.354	1.353	1.357	1.359
r(C7−F11)	1.346	1.355	1.349	1.349	1.353	1.352	1.354	1.355
∠(O1═C2−C3)	124.9	127.7	122.9	121.3	128.6	128.6	121.4	121.5
∠(C2−C3═C4)	119.5	125.1	132.8	131.6	125.6	125.2	133.5	133.5
∠(C3═C4−O5)	122.3	120.8	128.0	121.9	121.4	116.8	119.7	114.9
∠(C4−O5−H6)	106.9	109.6	111.7	110.0	109.9	109.7	109.8	109.9
∠(O1═C2−C7)	116.4	118.8	116.3	117.2	118.0	117.9	116.4	116.2
∠(O5−C4−C8)	113.8	116.3	110.4	115.8	111.3	116.2	109.6	114.4
∠(C2−C7−F9)	112.2	111.9	112.2	110.4	111.8	111.7	111.0	111.1
∠(C2−C7−F10)	110.6	110.3	110.9	111.1	110.6	110.6	110.8	110.9
∠(C2−C7−F11)	109.8	110.6	111.1	111.1	110.1	110.2	111.5	111.6
∠(C3═C4−O5−H6)	0.0	179.9	8.3	180.0	359.9	180.0	2.2	182.5
	ccc-F	*cct*-F	*tcc*-F	*tct*-F	*ctc*-F	*ctt*-F	*ttc*-F	*ttt*-F
ΔE^b	4.68	64.1	62.3	57.2	76.8	65.0	78.5	75.2
r(O1═C2)	1.245	1.221	1.222	1.223	1.220	1.222	1.225	1.225
r(C2−C3)	1.455	1.482	1.478	1.485	1.482	1.479	1.487	1.485
r(C3═C4)	1.361	1.346	1.348	1.343	1.350	1.348	1.349	1.347
r(C4−O5)	1.322	1.345	1.349	1.356	1.350	1.350	1.355	1.357
r(O5−H6)	1.009	0.973	0.970	0.972	0.972	0.973	0.972	0.971
r(C2−C7)	1.511	1.522	1.526	1.516	1.522	1.521	1.515	1.517
r(C4−C8)	1.518	1.518	1.520	1.516	1.534	1.533	1.527	1.526
r(C8−F9)	1.347	1.338	1.344	1.336	1.345	1.375	1.337	1.362
r(C8−F10)	1.344	1.348	1.346	1.348	1.341	1.333	1.351	1.345
r(C8−F11)	1.344	1.362	1.346	1.365	1.341	1.334	1.349	1.342
∠(O1═C2−C3)	121.1	123.1	119.4	118.2	123.7	123.4	116.5	116.8
∠(C2−C3═C4)	119.4	125.3	129.4	128.6	127.4	126.5	134.5	134.1
∠(C3═C4−O5)	125.1	124.8	129.8	124.7	123.7	119.6	123.1	118.6
∠(C4−O5−H6)	105.1	109.1	110.6	109.1	109.1	108.9	108.9	109.6
∠(O1═C2−C7)	120.3	121.7	120.0	121.4	121.4	121.4	120.3	120.0
∠(O5−C4−C8)	112.3	114.2	108.7	113.7	110.2	114.6	109.3	114.0
∠(C2−C8−F9)	111.4	113.1	112.0	113.2	110.2	108.0	111.5	109.6
∠(C2−C8−F10)	110.6	111.3	110.5	111.3	111.1	112.7	110.9	112.4
∠(C2−C8−F11)	110.6	109.3	110.5	109.1	111.1	112.7	111.3	112.7
∠(C3═C4−O5−H6)	0.0	191.6	0.0	194.4	0.0	180.0	359.3	177.0

[a] Other structural parameters are available upon request. [b] Relative energies.

These differences are understandable if the two intramolecular interactions proposed in HFAA[23] are taken into account in addition to the intramolecular hydrogen bonding in *ccc*: One is the stabilization due to the hydrogen bonding between the CF_3 and OH groups, represented by a broken line in Figure 1, and the other is the instability caused by the repulsion between the CF_3 group and the lone pairs of the C═O or C−O group. The former plays in F-*tcc*, *cct*-F, *tct*-F, *ctt*-F, and *ttt*-F, while the latter plays in F-*tct*, *ctc*-F, and *ctt*-F. The hydrogen atom in the O−H group for the F-*tcc*, *cct*-F, and *tct*-F isomers is out-of-plane, where the dihedral angle of C3═C4−O5−H6 is about 8−14° apart from 0 or 180°. On the other hand, the hydrogen atom for the *ctt*-F and *ttt*-F isomers is in-plane. The C−F distances related to the hydrogen bonding, 1.380, 1.362, 1.365, 1.375, and 1.362 Å for F-*tcc*, *cct*-F, *tct*-F, *ctt*-F, and *ttt*-F, respectively, are longer than the others, 1.33−1.35 Å. A similar discussion has been made by Buemi.[28]

Assignment of Infrared Spectra. *(1) ccc Isomer.* An infrared spectrum of TFAA in an argon matrix was recorded after sample deposition before UV irradiation. The C═O and C═C stretching bands appearing around 1600 cm^{-1} are slightly broadened even in the low-temperature condition, probably because of the intramolecular hydrogen bonding of C═O- - -H−O−C and π-electron conjugation. The intensities of the two bands are weaker than those of AA,[10] but stronger than those of HFAA.[24] The O−H stretching band, which is predicted to appear around 3038 cm^{-1}, has not been detected by broadening like AA and HFAA.

The calculated spectral patterns of the three stable isomers, F-*ccc*, *ccc*-F, and keto, are compared with the observed spectrum in Figure 2, where a scaling factor of 0.98 is used. It is found that the most stable isomer, F-*ccc*, reproduces the observed bands more satisfactorily than the others. The consistency between the observed and calculated wavenumbers summarized in Table 2 is slightly worse than those of the other molecules on which we reported previously, probably because TFAA contains multiple halogen atoms and intramolecular hydrogen bonding.[29,30]

According to the Boltzmann distribution law, the population ratio for the second stable isomer, *ccc*-F, and F-*ccc* can be estimated to be 13/87 if the calculated energy difference, 3.40 kJ mol^{-1}, is correct. However, no infrared bands for *ccc*-F have

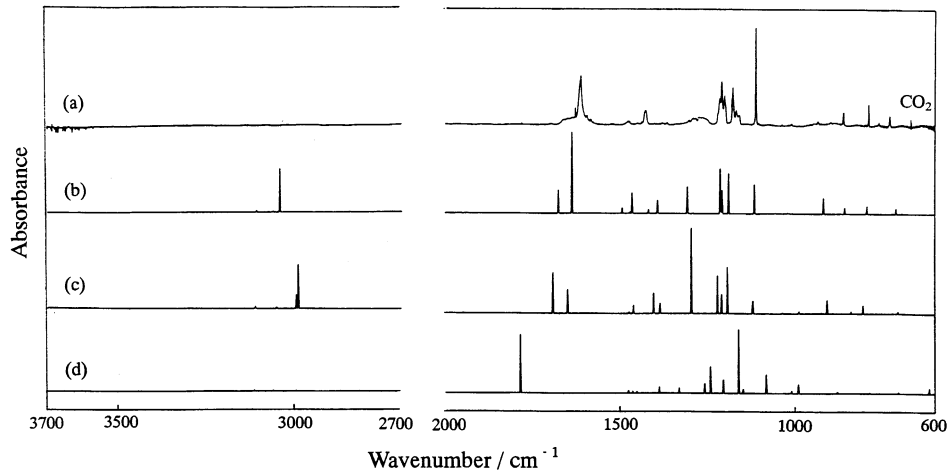

Figure 2. Comparison of infrared spectra of F-*ccc*, *ccc*-F, and keto isomers: (a) measured after deposition and before UV irradiation; (b) a spectral pattern of F-*ccc* calculated at the DFT/B3LYP/6-31G* level; (c) *ccc*-F; and (d) keto isomer. Most observed bands are assigned to the most stable chelated enol isomer, F-*ccc*.

TABLE 2: Observed and Calculated Wavenumbers (in cm^{-1}) of Enol Isomers of (Trifluoroacetyl)acetone[a]

F-*ccc*		F-*ctc*		*ctt*-F		*tct*-F		F-*ctt*	
obsd	calcd[b]	obsd	calcd[b]	obsd	calcd[b]	obsd	calcd[b]	obsd	calcd[b]
	3206 (w)	3588 (m)	3636 (w)	3610 (vs)	3641 (vs)	3604 (vs)	3650 (s)	3619 (s)	3665 (m)
	3104 (w)		3144 (w)		3132 (w)		3173 (w)		3156 (w)
	3057 (w)		3111 (w)		3107 (w)		3106 (w)		3130 (w)
	3038 (s)		3050 (w)		3042 (w)		3062 (w)		3025 (w)
	3001 (w)		2999 (w)		2987 (w)		3002 (w)		2975 (w)
1646 (w)	1673 (m)	1725 (m)	1753 (m)	1726 (s)	1757 (s)	1710 (w)	1732 (s)	1725 (m)	1750 (m)
1608 (s)	1634 (vs)	1617 (s)	1637 (vs)	1659 (vs)	1673 (vs)	1693 (s)	1716 (m)	1638 (vs)	1664 (vs)
1472 (w)	1491 (w)		1490 (w)		1473 (w)	1436 (w)	1473 (w)		1501 (w)
1436 (w)	1469 (w)		1473 (w)	1427 (w)	1466 (w)	1421 (w)	1459 (w)		1465 (w)
1423 (m)	1463 (m)	1447 (w)	1456 (w)	1400 (vs)	1424 (vs)	1394 (m)	1401 (m)	1426 (m)	1436 (m)
1378 (w)	1417 (w)	1370 (m)	1396 (w)	1360 (w)	1384 (w)	1366 (m)	1390 (w)		1396 (w)
1363 (w)	1391 (m)	1335 (w)	1338 (m)	1315 (m)	1321 (m)	1305 (w)	1317 (w)	1327 (s)	1332 (s)
1274 (w)	1306 (s)		1281 (w)	1252 (m)	1269 (s)	1259 (w)	1268 (m)	1269 (m)	1276 (m)
1208 (s)	1212 (vs)	1218 (w)	1230 (w)	1214 (vs)	1237 (vs)	1242 (vs)	1241 (vs)	1212 (s)	1223 (vs)
1200 (s)	1207 (m)	1195 (s)	1209 (s)	1189 (vs)	1194 (vs)	1217 (vs)	1221 (vs)	1202 (s)	1214 (m)
1176 (s)	1188 (s)	1147 (s)	1157 (s)	1149 (vs)	1161 (vs)	1142 (vs)	1150 (vs)	1151 (vs)	1161 (vs)
1110 (vs)	1114 (s)	1084 (s)	1090 (s)	1118 (m)	1101 (vs)	1078 (w)	1077 (w)	1077 (vs)	1081 (m)
1036 (w)	1055 (w)		1064 (w)	1017 (w)	1029 (w)	1026 (w)	1038 (w)		1062 (w)
1009 (w)	1019 (w)	1014 (w)	1025 (w)	954 (m)	950 (m)	996 (w)	995 (w)		1023 (w)
945 (w)	949 (w)	878 (s)	877 (m)	931 (w)	931 (m)	855 (w)	873 (w)	877 (s)	875 (s)
934 (w)	918 (m)		851 (w)	850 (w)	856 (w)	852 (w)	843 (w)	842 (m)	850 (w)
862 (m)	858 (w)	815 (w)	815 (w)	779 (w)	759 (w)	812 (w)	800 (w)		846 (w)
791 (m)	796 (w)		748 (w)	656 (w)	670 (w)	714 (w)	694 (w)		751 (w)
762 (w)	762 (w)	731 (w)	710 (w)		646 (w)		685 (w)		711 (m)
730 (m)	712 (w)								

[a] Relative intensities are in parentheses. Symbols in parentheses, vs, s, m, and w, represent very strong, strong, medium, and weak, respectively. [b] Calculated at the DFT/B3LYP/6-31G* level. A scaling factor of 0.98 is used. Calculated wavenumbers and relative intensities for other vibrational modes and other isomers are available upon request.

been observed in Figure 2a; for example, the strongest band predicted to appear around 1300 cm^{-1} is not found in the observed spectrum. A few peaks of the bands appearing around 1100 cm^{-1} may be assigned to *ccc*-F, but it is more reasonable to assume that they are caused by the matrix effect or Fermi resonance in the F-*ccc* bands. Even when the temperature of the deposition nozzle was elevated from 300 to 450 K to increase the population ratio of *ccc*-F/F-*ccc* from 13/87 to 22/78, no spectral change was observed. Thus we assume that the conformational change from the less stable *ccc*-F to the more stable F-*ccc* occurs in the matrix by hydrogen atom tunneling. The importance of tunneling in the conformational dynamics of O—H groups has been pointed out in similar studies of formic acid[31−33] and hydroquinone derivatives.[14,18]

The C═O stretching modes for the keto isomer are expected to appear around 1800 cm^{-1}. One of them, the asymmetric stretching mode, must have a high infrared intensity. However, no band appears in this region, implying that the keto form of TFAA, the relative energy of which is estimated to be higher than that of F-*ccc* by 21.2 kJ mol^{-1}, is negligible in the gas phase and the argon matrix.

(2) F-ctc Isomer. When the matrix sample was exposed to the UV light from a superhigh-pressure mercury lamp through UV28 short-cut and water filters ($\lambda > 280$ nm), a spectral change was observed. A difference spectrum between those measured before and after the 240-min UV irradiation is shown in Figure 3a. Decreasing and increasing bands are due to the reactant F-*ccc* and photoproducts, respectively. Since six bands of the photoproducts are observed in the C═O and C═C stretching regions, it is expected that at least three isomers are produced from the F-*ccc* isomer by UV irradiation. After the measurement of Figure 3a, we exposed the matrix sample to the UV light through UV32

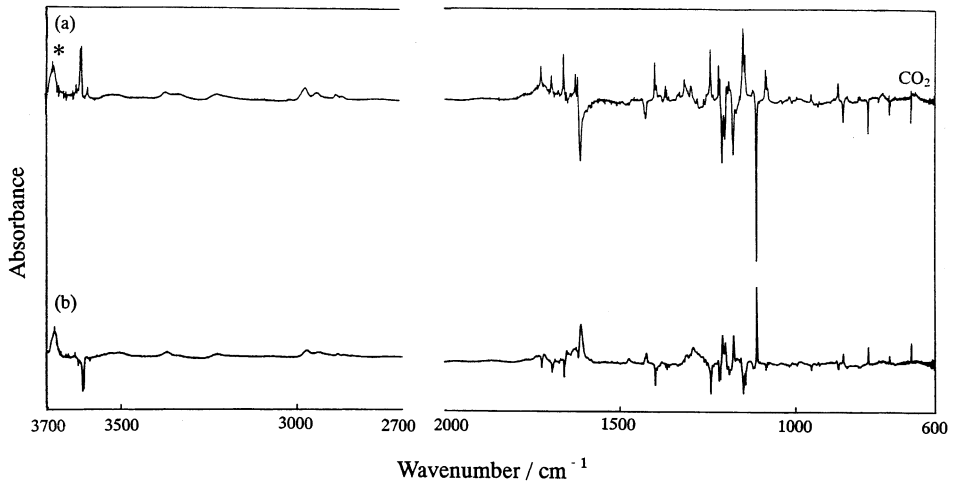

Figure 3. Difference infrared spectra: (a) after minus before 240-min UV28 irradiation ($\lambda > 280$ nm) and (b) after minus before 180-min UV32 irradiation ($\lambda > 320$ nm) subsequent to the 240-min UV28 irradiation in part a. This photoisomerization is completely reversible. The band identified by the asterisk may be due to an impurity of water in the matrix.

short-cut and water filters ($\lambda > 320$ nm) and found a reversible spectral change, as shown in Figure 3b, where the intensities of the F-*ccc* bands increase and those of the photoproduct bands decrease. This finding supports that nonchelated enol isomers are produced from F-*ccc* by rotational isomerization after destruction of the intramolecular hydrogen bonding. Similar phenomena observed in our previous studies of AA[10] and HFAA[23,24] led to the conclusion that conformational isomerization around the three rotational axes occurred reversibly.

The observed bands of the nonchelated enol isomers can be classified into three groups by using irradiation-time and -wavelength dependences of the band intensities, as in the identification of nonchelated enol isomers of AA and HFAA. Figure 4a shows a difference spectrum between those measured before and after the 4-min UV28 irradiation, where the bands exhibiting the same growth behavior are extracted by computational subtraction of the other photoproduct bands. This isomer is produced more rapidly than the other nonchelated enol isomers upon UV28 irradiation. By a comparison of the observed spectrum with spectral patterns of all the nonchelated isomers obtained by the DFT calculation, it was assignable to F-*ctc*. The calculated spectral pattern of F-*ctc* is compared with the observed spectrum in Figure 4a. Their vibrational wavenumbers are summarized in Table 2. The C═O and C═C stretching modes are observed at 1725 and 1617 cm^{-1}, which are consistent with the corresponding calculated values, 1753 and 1637 cm^{-1}, respectively. The small differences between the observed and calculated wavenumbers can be ascribed to the intrinsic inaccuracy of the calculations. The O—H stretching band, which is undetectable in the F-*ccc* spectrum by the band broadening due to intramolecular hydrogen bonding, is clearly observed at 3588 cm^{-1}. This finding supports our conclusion that this isomer produced by the UV irradiation is one of the nonchelated enol forms. The consistency between the observed and calculated spectra is better than that of the reactant, F-*ccc*.

(3) ctt-F Isomer. A similar spectral analysis has been made for another isomer. Figure 4b shows a difference spectrum between those measured before and after the 310-min UV30 irradiation, where the other nonchelated isomer bands are subtracted computationally. This observed spectrum is found to be consistent with the spectral pattern of *ctt*-F shown in Figure 4b. The C═O and C═C stretching modes appear at 1726 and 1659 cm^{-1}, which are consistent with the corresponding calculated values, 1757 and 1673 cm^{-1}. The relative intensities are also reproduced satisfactorily. The consistency between the observed and calculated wavenumbers for *ctt*-F, summarized in Table 2, is similar to that for F-*ctc* and better than that for F-*ccc*. The O—H stretching mode predicted to appear at 3641 cm^{-1} is clearly observed at 3610 cm^{-1}.

(4) tct-F Isomer. The infrared spectrum of the *tct*-F isomer can also be extracted from a spectrum measured without short-cut filters. A difference spectrum between those measured before and after the 42-min UV irradiation is shown in Figure 4c. The C═O and C═C stretching bands appear at 1710 and 1693 cm^{-1}, which are consistent with the corresponding calculated values of *tct*-F, 1732 and 1716 cm^{-1}. The relative intensities of the observed bands are inconsistent with the calculated ones. The accuracy of the DFT calculation is insufficient to make a quantitative estimate of the intensities for bands composed of two mixing vibrational modes with a small wavenumber difference. Other than the relative intensities, the calculated spectral pattern reproduces the observed spectrum satisfactorily. The observed and calculated wavenumbers are summarized in Table 2. The O—H stretching mode is observed at 3604 cm^{-1}, which is nearly equal to that of *ctt*-F. Both isomers have intramolecular hydrogen bonding of CF_3- - -H—O—C.

As for AA, an infrared spectrum of the keto isomer was observed when either the matrix sample was irradiated without short-cut filters or the deposition nozzle was heated. However, no infrared bands of the keto isomer for TFAA have been observed, as in the case of HFAA.

(5) Transient Species, F-ctt Isomer. Our experimental system can measure infrared spectra of the transient species produced during UV irradiation. Using this system, we have observed infrared spectra of electronically excited triplet states for naphthalene,[34] 1,2- and 1,4-dicyanobenzenes,[35] tetracyanobenzene,[36] tetracyanopyrazine,[36] tetrafluoropyrazine,[36] and 1,4-dicyano-2,3,5,6-tetrafluorobenzene.[37] We have tried to measure infrared spectra of the transient nonchelated enol isomers produced during UV-30 irradiation in the present study. The matrix sample was exposed to the UV light while an IR spectrum was recorded. In addition to the bands assigned to the three nonchelated enol isomers, F-*ctc*, *ctt*-F, and *tct*-F, we were able to observe transient infrared bands, which immediately disappeared after termination of the irradiation. The difference spectrum between those measured before and during the UV irradiation is shown in Figure 4d, where the bands for the stable photoproducts are subtracted computationally. The decreasing

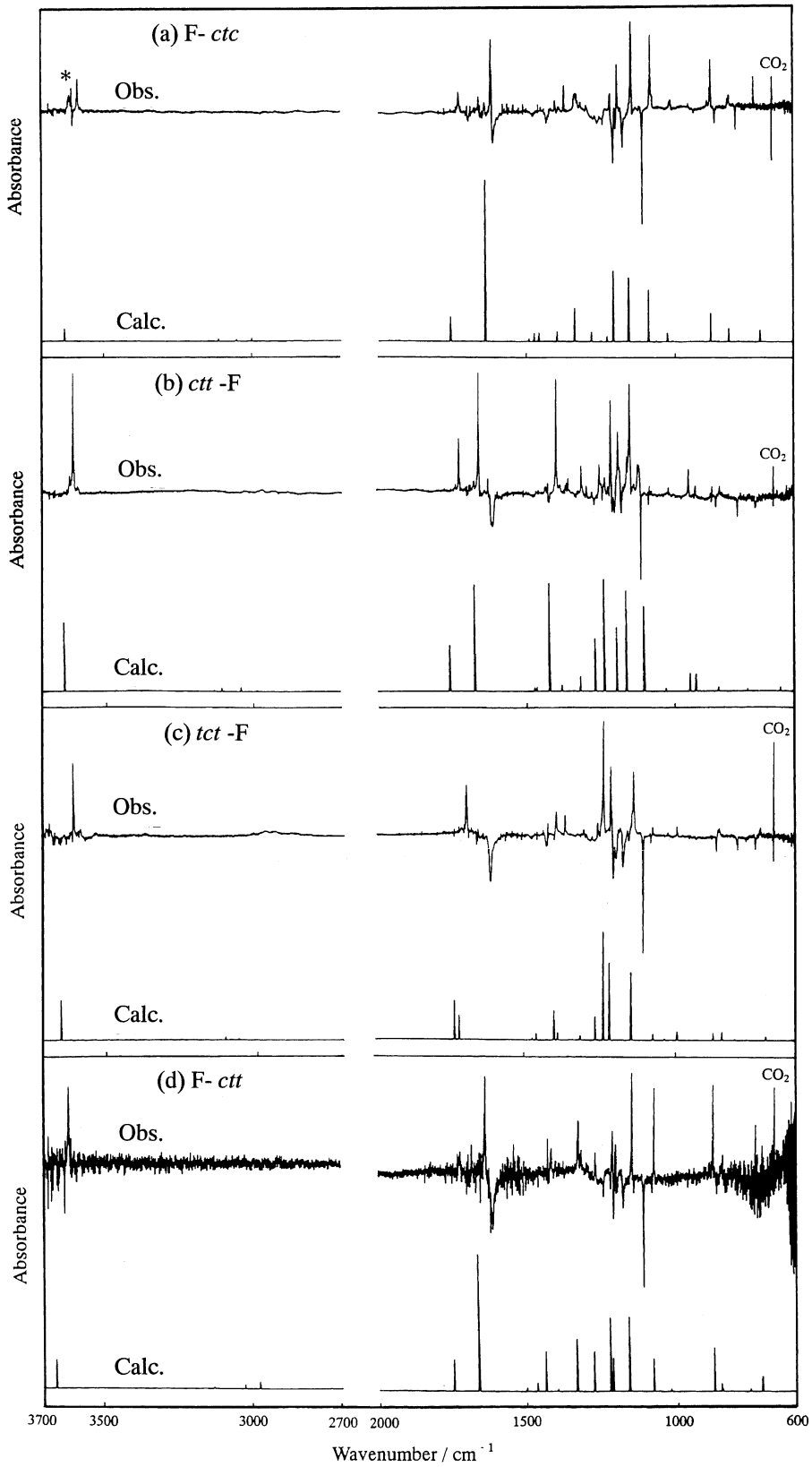

Figure 4. Observed matrix-isolation infrared spectra (upper) and calculated spectral patterns (lower) obtained at the DFT/B3LYP/6-31G* level of enol-type (trifluoroacetyl) acetone: (a) F-*ctc*, difference between the spectra measured before and after 4-min UV28 irradiation (λ > 280 nm); (b) *ctt*-F, difference between the spectra measured before and after 310-min UV30 irradiation (λ > 300 nm); (c) *tct*-F, difference between the spectra measured before and after UV irradiation without optical filters for 42 min; (d) a transient species F-*ctt*, difference between the spectra measured before and during UV30 irradiation. Bands for other nonchelated isomers in the observed spectra are subtracted computationally. The band identified by the asterisk may be due to an impurity of water in the matrix.

bands are due to a reactant, F-*ccc*. The observed transient spectrum is consistent with the calculated spectral pattern of F-*ctt*. The C═O and C═C stretching bands appear at 1725 and 1638 cm^{-1}, which correspond to the calculated values, 1750

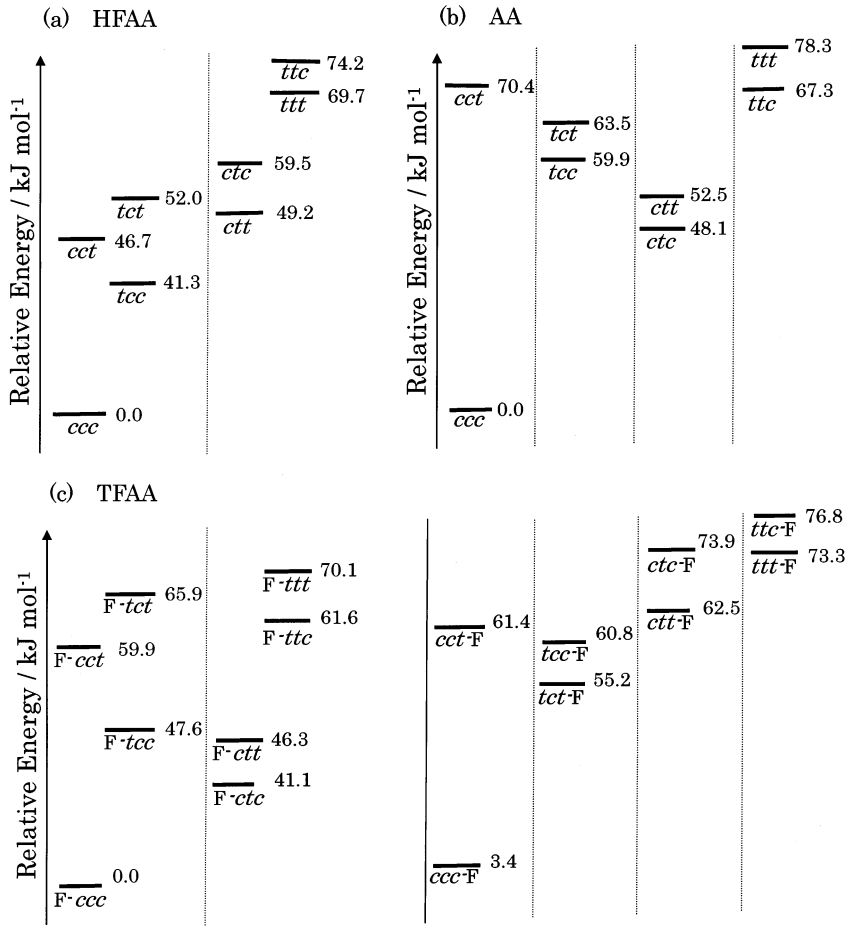

Figure 5. Relative energies (in kJ mol^{-1}) calculated at the DFT/B3LYP/6-31G* level after zero-point vibrational corrections: (a) hexafluoroacetylacetone (HFAA);[23] (b) acetylacetone (AA);[10] and (c) (trifluoroacetyl)acetone (TFAA). Dotted lines represent inhibition of rotational isomerization around the C3═C4 bond for HFAA and F-*xxx* of TFAA, and around the C3═C4 and C2─C3 bonds for AA and *xxx*-F of TFAA.

and 1664, cm^{-1}, respectively. The observed and calculated wavenumbers of this isomer are summarized in Table 2. The O─H stretching band, observed at 3619 cm^{-1}, is 30 cm^{-1} higher than that of F-*ctc*, being consistent with the corresponding calculated one, 29 cm^{-1}.

Mechanism of Photoisomerization. *(1) Comparison with AA and HFAA.* In the case of HFAA, only the *ctt* isomer is produced from *ccc*. To explain this selective conformational change, we proposed the following reaction mechanism:[23] (1) The reactant, *ccc*, is excited to the $\pi\pi^*$ transition state of C3═C4 by UV irradiation. (2) Since the C3═C4 bond has single-bond character in the excited state, rotational isomerization takes place around this bond and produces vibrationally hot central trans enol isomers, *ctc*, *ttc*, *ctt*, and *ttt*. (3) Isomerizations around the C2─C3 and C4─O5 single bonds occur in thermal relaxation, producing the most stable isomer among the four, *ctt*. (4) Other nonchelated central cis enol isomers, *tcc*, *cct*, and *tct*, are converted to the original isomer, *ccc*, in relaxation, even if they are produced in the photoexcitation process. Then we have observed the most stable isomer in each group, divided by a dotted line in Figure 5a, *ccc* and *ctt*.

This reaction mechanism can explain the photoisomerization of AA, where the *ctc*, *tct*, and *ttc* nonchelated isomers are produced from *ccc*, but not *cct*, *ctt*, *tcc*, and *ttt*. We assume that the isomerization around the C2─C3 bond is inhibited in thermal relaxation like C3═C4, because the π-electron conjugation in AA is stronger than that in HFAA. Then eight enol isomers are classified into four groups by inhibition of the isomerization around the C3═C4 and C2─C3 bonds, as shown in Figure 5b. This scheme accounts for our observation of the IR spectra of the more stable isomers: *ccc*, *ctc*, and *ttc* in each group. The reason the IR spectrum of *tct*, which is less stable than *tcc*, was exceptionally observed instead of *tcc* was ascribed in our paper[23] to the steric effect of the methyl group.

The mechanism discussed above is applicable to TFAA, where F-*ctc*, *ctt*-F, and *tct*-F are produced from F-*ccc*. First, the 16 enol isomers are divided into two groups, F-*xxx* and *xxx*-F, as shown in Figure 5c. The F-*xxx* group is further divided into the central cis and central trans groups by inhibition of the isomerization around the C3═C4 bond, like HFAA. As a result, we can account for the observation of the IR spectra of the most stable enol isomers in each group: F-*ccc* and F-*ctc*. On the other hand, the *xxx*-F group is further divided into four groups by inhibition of the isomerization around the C3═C4 and C2─C3 bonds, like AA. Then, we should be able to observe the IR spectra of the more stable isomer in each group, i.e., *ccc*-F, *tct*-F, *ctt*-F, and *ttt*-F. Among the four isomers, however, we have not been able to observe any bands assignable to *ttt*-F in the complicated spectra. The most stable isomer in the *xxx*-F group, *ccc*-F, is probably isomerized immediately to F-*ccc* by the hydrogen atom tunneling between the H─O and C═O groups, as discussed above. This assumption may be confirmed by a similar experiment with deuterated species, but we have not yet been successful. On the other hand, we have also observed the IR spectrum of a transient nonchelated enol, F-*ctt*. This isomer is probably produced directly from F-*ccc* and/or via the less stable isomers, F-*ttt* and F-*ttc*, by the UV irradiation,

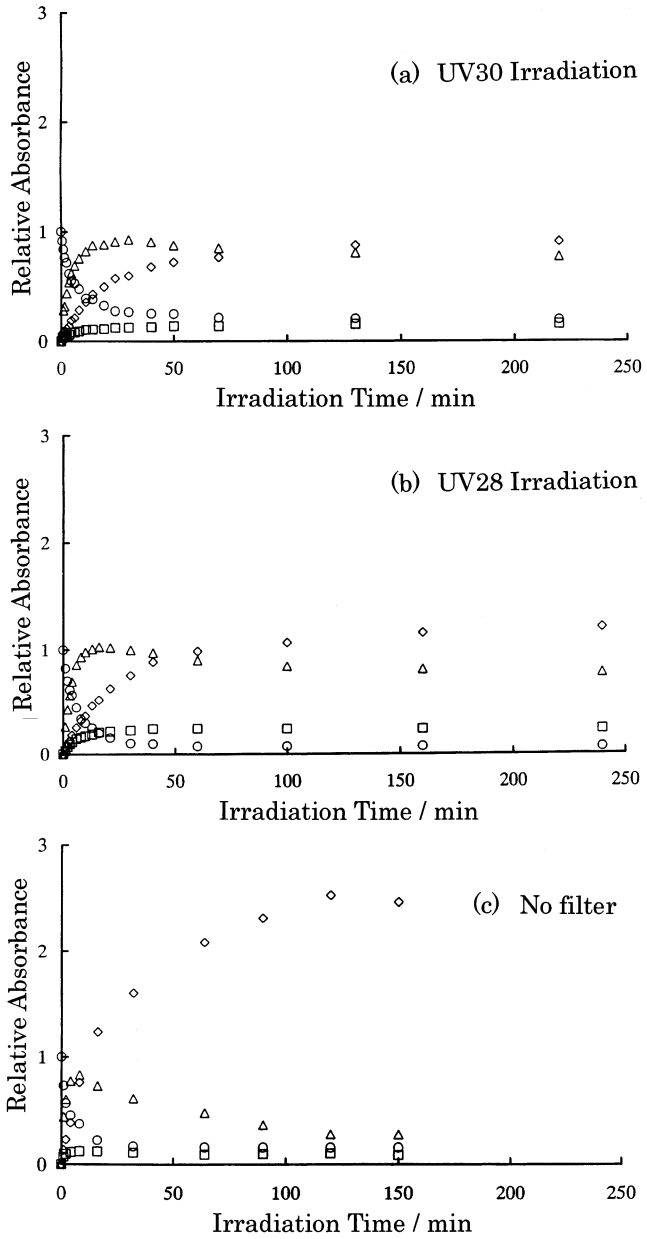

Figure 6. Irradiation-time dependence of absorbance of the 791-, 878-, 954-, and 1693-cm^{-1} bands for F-*ccc* (○), F-*ctc* (△), *ctt*-F (□), and *tct*-F (◇), respectively: (a) UV30 irradiation; (b) UV28 irradiation; and (c) no filter.

and then isomerized to F-*ctc* by a conformational change around the C4—O5 bond immediately after termination of the irradiation.

(2) Dependence of Absorbance on Irradiation Time. More detailed information on the photoisomerization mechanism can be derived from the dependence of the absorbance on the irradiation time. Figure 6 shows absorbance changes of the 791-, 878-, 954-, and 1693-cm^{-1} bands for F-*ccc*, F-*ctc*, *ctt*-F, and *tct*-F, respectively, where the absorbance values are normalized by using that of the F-*ccc* band measured before UV irradiation to make the amount of matrix samples constant. The absorbance changes measured upon UV30 irradiation (Figure 6a) show that the F-*ctc* band (△) increases rapidly in the beginning and then decreases slightly, whereas the *tct*-F band (◇) increases slowly and continuously upon irradiation. These findings suggest that the *tct*-F isomer is produced from the F-*ctc* isomer by a second photon. This trend was observed more clearly when the matrix sample was exposed to the UV light through a UV28 short-cut

SCHEME 2

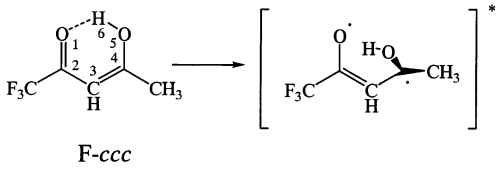

filter (Figure 6b) and without short-cut filters (Figure 6c), where F-*ctc* and *tct*-F behave like an intermediate and a final product due to a two-stepwise two-photon reaction, respectively. An induction period of the *tct*-F band is certainly observed in the beginning of UV irradiation. This second-photon isomerization from F-*ctc* to *tct*-F is accelerated by the shorter wavelength irradiation.

On the other hand, the *ctt*-F band (□) increases rapidly and becomes constant in a short time upon UV irradiation. No induction period is observed upon irradiation at any wavelength. This means that the *ctt*-F isomer is directly produced from the F-*ccc* isomer by one photon. The relative amount of *ctt*-F (□) measured without short-cut filters is smaller than that measured upon UV28 irradiation, probably because the major branching reaction to produce F-*ctc* from F-*ccc* is more accelerated as the irradiation wavelength becomes shorter. The reactant, F-*ccc* (○), decreases exponentially but does not tend to zero, probably because F-*ccc* is in equilibrium with other nonchelated enol isomers at the infinite irradiation time like HFAA.

(3) Mechanism of First-Photon Isomerization. With the aid of the above-mentioned dependence of the absorbance on the irradiation time, we conclude that the first photoisomerization yields F-*ctt* (a transient species produced during the UV irradiation), F-*ctc* (a precursor of *tct*-F), and *ctt*-F (a final product) from the most stable isomer, F-*ccc*. All these products commonly have cis conformation around the C2—C3 bond, i.e., the first italic letter is *c*. To explain this fact, we assume a perpendicular structure in the $\pi\pi^*$ transition state of C3═C4 caused by UV irradiation (Scheme 2): The C3═C4 bond has single-bond character, while the C2—C3 bond has double-bond character. Therefore, the conformational changes around the C3═C4 bond occur keeping the cis conformation around the C2—C3 bond and produce the F-*cct*, F-*ctc*, and F-*ctt* isomers. The F-*cct* isomer, whose relative energy is 61.9 kJ mol^{-1} higher than that of F-*ccc*, is immediately isomerized to F-*ccc* by the conformational change around C4—O5 in thermal relaxation. Similarly F-*ctt*, which has an infrared spectrum observable during UV irradiation, is isomerized to F-*ctc* by the same conformational change. If the UV-induced conformational changes occur with the hydrogen atom moving from O—H to C═O, the *cct*-F, *ctc*-F, and *ctt*-F isomers might be produced from *ccc*-F in the *xxx*-F group. Similarly to the F-*xxx* group, *cct*-F and *ctc*-F change to *ccc*-F and *ctt*-F, respectively, by the conformational changes around C4—O5 in thermal relaxation. This scheme explains why we have observed the infrared spectrum of *ctt*-F, but not that of *ccc*-F, which changes to F-*ccc* by hydrogen atom tunneling as described above. The first-photon isomerization mechanism is summarized in Scheme 3.

(4) Mechanism of Second-Photon Isomerization. In the second-photon isomerization, F-*ctc*, which is the most stable isomer among the nonchelated F-*xxx* isomers, changes to *tct*-F, which is the most stable isomer among the nonchelated *xxx*-F isomers. To produce *xxx*-F from F-*xxx*, the hydrogen atom in the OH group must move to the C═O group. This transfer readily occurs between the chelated enol isomers, F-*ccc* and *ccc*-F, in the electronic ground (S_0) states but is difficult between

SCHEME 3

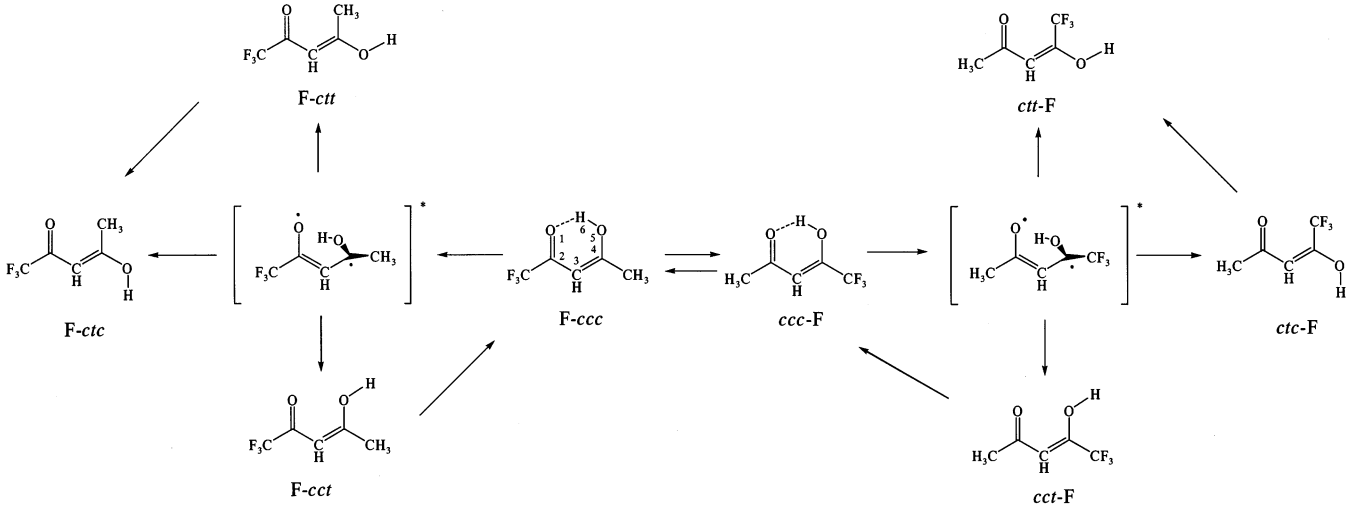

SCHEME 4

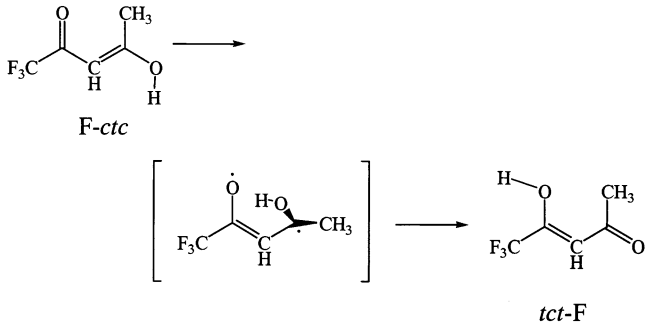

the nonchelated isomers in the S_0 states because the hydrogen atom in the OH group is separated far from the C═O group. In contrast, the hydrogen atom may approach the C═O group in the electronically excited state of the F-*ctc* isomer, where the O−H group is perpendicular to the C═O group (Scheme 4). Then the F-*ctc* isomer changes to nonchelated *xxx*-F isomers upon UV irradiation, and finally to the most stable nonchelated enol isomer in the *xxx*-F group, i.e., *tct*-F.

Note that this conformational change never occurs in the first-photon isomerization, although the structure of the electronically excited state of these processes is identical. To explain this fact, we must assume that the photoexcitation energy from F-*ccc* is insufficient to surmount the barrier to yield *tct*-F in the electronically excited state, while it is sufficient to surmount that for F-*ctc*, whose relative energy is 42.4 kJ mol^{-1} higher than that of F-*ccc*. The F-*ctc* isomer plays the role of a ledge in the production of the final product *tct*-F.

Summary

An infrared spectrum of TFAA in an argon matrix has been measured with an FTIR spectrophotometer. The observed bands are assigned to F-*ccc*, but not to *ccc*-F or keto isomers, with the aid of DFT calculations. Hydrogen atom tunneling resulting in the conformational change from *ccc*-F to F-*ccc* is proposed on the basis of the experimental results which use a high-temperature nozzle. Infrared spectra of nonchelated isomers produced upon UV irradiation have also been measured. The observed dependence of the absorbance on the irradiation time results in the assignment of three nonchelated enol isomers to F-*ctc*, *ctt*-F, and *tct*-F, which are the most stable ones in each group, being hindered by barriers of internal rotation caused by π-electron conjugation. A conformational change from F-*ctc* to *tct*-F induced by the second-photon irradiation and accelerated by the shorter wavelength irradiation has been observed. An infrared spectrum of another nonchelated isomer produced during irradiation has also been measured and assigned to F-*ctt*.

Acknowledgment. The authors wish to thank Professor Kozo Kuchitsu (Tokyo University of Agriculture and Technology) for his helpful discussion.

References and Notes

(1) Veillon, C.; Patterson, K. Y.; Moser-Veillon, P. B. *J. Anal. At. Spectrosc.* **1996**, *11*, 727.
(2) Lin, Y.; Wai, C. M. *Anal. Chem.* **1994**, *66*, 1971.
(3) Nakanishi, H.; Morita, H.; Nagakura, S. *Bull. Chem. Soc. Jpn.* **1977**, *50*, 2255.
(4) Lazaar, K. I.; Bauer, S. H. *J. Phys. Chem.* **1983**, *87*, 2411.
(5) Folkend, M. M.; Weiss-Lopez, B. E.; Chuvel, J. P.; True, N. S. *J. Phys. Chem.* **1985**, *89*, 3347.
(6) Schieringand, D. W.; Katon, J. E. *Appl. Spectrosc.* **1986**, *40*, 1049.
(7) Bauer, S. H.; Wilcox, C. F. *Chem. Phys. Lett.* **1997**, *279*, 122.
(8) Roubin, P.; Chiavassa, T.; Verlaque, P.; Pizzala, L.; Bodot, H. *Chem. Phys. Lett.* **1990**, *175*, 655.
(9) Chiavassa, T.; Verlaque, P.; Pizzala, L.; Roubin, P. *Spectrochim. Acta* **1994**, *50A*, 343.
(10) Nagashima, N.; Kudoh, S.; Takayanagi, M.; Nakata, M. *J. Phys. Chem. A* **2001**, *105*, 10832.
(11) Labanowski, J.; Andzelm, J. W., Eds. *Density Functional Methods in Chemistry*; Springer-Verlag: New York, 1991.
(12) Seminario, J. M.; Politzer, P., Eds. *Modern Density Functional Theory*: *A Tool for Chemistry*; Elsevier: Amsterdam, The Netherlands, 1995.
(13) Uechi, T.; Kudoh, S.; Takayanagi, M.; Nakata, M. *J. Phys. Chem.* **2002**, *106*, 3365.
(14) Akai, N.; Kudoh, S.; Takayanagi, M.; Nakata, M. *Chem. Phys. Lett.* **2002**, *356*, 133.
(15) Futami, Y.; Kudoh, S.; Takayanagi, M.; Nakata, M. *Chem. Phys. Lett.* **2002**, *353*, 209.
(16) Akai, N.; Kudoh, S.; Takayanagi, M.; Nakata, M. *J. Photochem. Photobiol. A* **2002**, *150*, 95.
(17) Akai, N.; Kudoh, S.; Takayanagi, M.; Nakata, M. *Chem. Phys. Lett.* **2002**, *363*, 591.
(18) Akai, S.; Kudoh, S.; Takayanagi, M.; Nakata, M. *J. Phys. Chem.* **2002**, *106*, 11029.
(19) Futami, Y.; Chin, M. C.; Kudoh, S.; Takayanagi, M.; Nakata, M. *Chem. Phys. Lett.* **2003**, *370*, 460.
(20) Akai, N.; Kudoh, S.; Nakata, M. *J. Phys. Chem. A* **2003**, *107*, 2635.
(21) Akai, N.; Kudoh, S.; Nakata, M. *J. Phys. Chem. A* **2003**, *107*, 6725.
(22) Coussan, S.; Manca, C.; Ferro, Y.; Roubin, P. *Chem. Phys. Lett.* **2003**, *370*, 118.
(23) Nagashima, N.; Kudoh, S.; Nakata, M. *Chem. Phys. Lett.* **2003**, *374*, 59.
(24) Nagashima, N.; Kudoh, S.; Nakata, M. *Chem. Phys. Lett.* **2003**, *374*, 67.

(25) Frisch, M. J.; Trucks, G. W.; Schlegel, H. B.; Scuseria, G. E.; Robb, M. A.; Cheeseman, J. R.; Zakrzewski, V. G.; Montgomery, J. A., Jr.; Stratmann, R. E.; Burant, J. C.; Dapprich, S.; Millam, J. M.; Daniels, A. D.; Kudin, K. N.; Strain, M. C.; Farkas, O.; Tomasi, J.; Barone, V.; Cossi, M.; Cammi, R.; Mennucci, B.; Pomelli, C.; Adamo, C.; Clifford, S.; Ochterski, J.; Petersson, G. A.; Ayala, P. Y.; Cui, Q.; Morokuma, K.; Malick, D. K.; Rabuck, A. D.; Raghavachari, K.; Foresman, J. B.; Cioslowski, J.; Ortiz, J. V.; Stefanov, B. B.; Liu, G.; Liashenko, A.; Piskorz, P.; Komaromi, I.; Gomperts, R.; Martin, R. L.; Fox, D. J.; Keith, T.; Al-Laham, M. A.; Peng, C. Y.; Nanayakkara, A.; Gonzalez, C.; Challacombe, M.; Gill, P. M. W.; Johnson, B.; Chen, W.; Wong, M. W.; Andres, J. L.; Head-Gordon, M.; Replogle, E. S.; Pople, J. A. *Gaussian 98*, revision A.6; Gaussian, Inc.: Pittsburgh, PA, 1998.

(26) Becke, A. D. *J. Chem. Phys.* **1993**, *98*, 5648.

(27) Lee, C.; Yang, W.; Parr, R. G. *Phys. Rev.* **1988**, *37B*, 785.

(28) Buemi, G. *J. Mol. Struct. THEOCHEM* **2000**, *499*, 21

(29) Yoshida, H.; Ehara, H.; Matsuura, H. *Chem. Phys. Lett.* **2000**, *325*, 477.

(30) Akai, N.; Kudoh, S.; Nakata, M. *J. Phys. Chem. A* **2003**, *107*, 3655.

(31) Pettersson, M.; Macoas, E. M. S.; Khriachtchev, L.; Fausto, R.; Räsänen, M. *J. Am. Chem. Soc.* **2003**, *125*, 4058.

(32) Pettersson, M.; Lundell, J.; Khriachtchev, L.; Räsänen, M. *J. Am. Chem. Soc.* **1997**, *119*, 11715.

(33) Pettersson, M.; Macoas, E. M. S.; Khriachtchev, L.; Lundell, J.; Fausto, R.; Räsänen, M. *J. Chem. Phys.* **2002**, *117*, 9095.

(34) Nakata, M.; Kudoh, S.; Takayanagi, M.; Ishibashi, T.; Kato, C. *J. Phys. Chem. A* **2000**, *104*, 11304.

(35) Akai, N.; Kudoh, S.; Nakata, M. *Chem. Phys. Lett.* **2003**, *371*, 655.

(36) Akai, N.; Miura, I.; Kudoh, S.; Shigehara, K.; Nakata, M. *Bull. Chem. Soc. Jpn.* **2003**, *76*, 1927.

(37) Akai, N.; Negishi, D.; Kudoh, S.; Takayanagi, M.; Nakata, M. *J. Mol. Struct.* **2004**, *688*, 177.